Micromagnetic study of spin-transfer-torque switching of a ferromagnetic cross towards multi-state spin-transfer-torque based random access memory

Urmimala Roy,[1,a)] Tanmoy Pramanik,[1] Maxim Tsoi,[2] Leonard F. Register,[1] and Sanjay K. Banerjee[1]
[1]*Microelectronics Research Center, The University of Texas at Austin, Austin, Texas 78758, USA*
[2]*Department of Physics, The University of Texas at Austin, Austin, Texas 78712, USA*

(Received 22 April 2013; accepted 30 May 2013; published online 13 June 2013)

We study spin-transfer-torque (STT) switching of a cross-shaped ferromagnet with unequal branches as the free layer in a magnetic tunnel junction using micromagnetic simulations. The free layer in the magnetic tunnel junction is thus designed to have four stable energy states using shape anisotropy. Switching shows distinct regions with increasing current density. Stability of the states against thermal fluctuations is considered, and the validity of the results for different dimensions and material parameters of the free layer ferromagnet is investigated. The results could be useful for a multi-bit STT-based memory. © *2013 AIP Publishing LLC*. [http://dx.doi.org/10.1063/1.4811230]

I. INTRODUCTION

Spin-transfer-torque-based random access memory (STTRAM)[1–4] is a promising candidate for nonvolatile memory with respect to scalability, power consumption, and access speed.[4] In an STTRAM cell, the logical value of the memory bit is stored as orientation of magnetic moment in its "free" layer. The bit typically consists of two ferromagnetic (FM) layers separated by an insulating tunnel barrier as in a magnetic tunnel junction (MTJ) structure. One of the two FM layers has fixed magnetization direction, while the other layer is free to be switched. In a typical MTJ device, the FM-tunnel barrier-FM stack has elliptic cross section, so that the free layer has an easy axis along the longer of the two axes of the ellipse, owing to shape anisotropy. Thus, it can be switched between the two minima in its energy landscape, corresponding to the two opposite directions of its magnetization along its easy axis. An STTRAM memory cell typically consists of a MTJ along with a selection transistor. Currently, the high switching current densities ($10^7 - 10^8$ A/cm^2) required to switch the bit using the STT effect is limiting the information storage density in this technology, as the required area of the transistor becomes very large.[5] In this paper, we consider the possibility of storing two memory bits within a single MTJ with a cross-shaped free layer that could still be addressed by one selection transistor. The studied STTRAM structure is similar to that reported in a recent patent.[6] In this work, however, we provide a detailed discussion of the switching dynamics and associated regions of reliable switching currents, in addition to illustrating the effects of varying device geometry on the latter. Other proposals of multi-bit STTRAM devices include multiple MTJs connected in series[7] or two different domains in the free layer switching at two different current densities.[8]

With two long branches in the free layer of the considered MTJ structures, there are an associated four valleys in the energy landscape. The angular positions of the free layer magnetization in these stable positions with respect to the fixed layer are designed so that the resistance of the MTJ has distinct values when the free layer magnetization resides in each of these valleys. Using micromagnetic simulations, we show switching between energy valleys using spin polarized current. We engineer the energy barrier between valleys by controlling the size of the branches.

The paper is organized as follows. In Secs. II and III, we analyze the stable states and switching among them via micromagnetic simulations, while addressing the effects of dimensions of and asymmetry between the arms of the cross in the free layer. In Sec. II, specifically, the four stable states of a representative cross-shaped free FM layer are discussed. In Sec. III, magnetization dynamics under spin-polarized current injection consistent with the assumed fixed layer orientation is discussed, and studies of effects of different dimensions and material parameters of the free layer are discussed. In Sec. IV, we comment on thermal stability of the cell.

II. STABLE MAGNETIZATION CONFIGURATIONS OF THE FREE LAYER FM

A cross-shaped free layer should have 2 easy axes, that is, 4 stable magnetization configurations. We confirm this using micromagnetic simulations (Figure 1). In the simulated structure, the short arms of the cross are each 40 nm along the longer axis and 20 nm wide in the other direction. The long arms are each 60 nm along the longer axis and 20 nm along the shorter axis. That makes the central part a 20 nm by 20 nm square. The thickness of the cross is assumed to be 2 nm. The magnetization is saturated along a direction, making a very small angle with the branches applying a large enough magnetic field, and then relaxed back to zero magnetic field. The magnetization relaxes to the configurations as shown in Figures 1(a)–1(d). These four states have equal energy barriers between them for a symmetric cross. Here, however, we make the two branches of the cross to be of unequal lengths. As the magnetization relaxes to these

a)urmimala@utexas.edu.

configurations with no magnetic field applied externally, these correspond to the minima of the energy landscape. Here we simulate the free layer FM alone. That is, we ignore any dipolar field from the fixed FM. This can be achieved in a real MTJ device using a synthetic antiferromagnet as the fixed layer.[9]

The material parameters used are saturation magnetization $M_s = 1400 \times 10^3$ A/m and uniform exchange constant $A = 30 \times 10^{-12}$ J/m, which are typical for cobalt.[10] We do not include any crystalline anisotropy so as to engineer the easy axes of the free magnet using shape anisotropy only. The shape anisotropy of the branches and hence the barrier height between the minima are effectively controlled by the aspect ratio (AR) of the branches for a given volume. The shape anisotropy of a FM depends on its demagnetization tensor. For an ellipsoid of a given AR the demagnetization tensor can be determined from Osborn's work.[11] For any geometry, other than an ellipsoid, this does not hold true.

III. MAGNETIZATION DYNAMICS INCLUDING STT

The resistance of the MTJ stack is a function of the cosine of the angle between the free layer and fixed layer magnetizations. So we propose to pin the fixed layer magnetization at around 22.5° with respect to the short branch. This serves to provide four different cosine values of the equilibrium magnetization directions of the central part of the cross with respect to the fixed layer magnetization direction and, hence, four different resistance values. This approach is similar to using non-collinear magnetizations in free and fixed layers of a MTJ or spin-valve.[12–15]

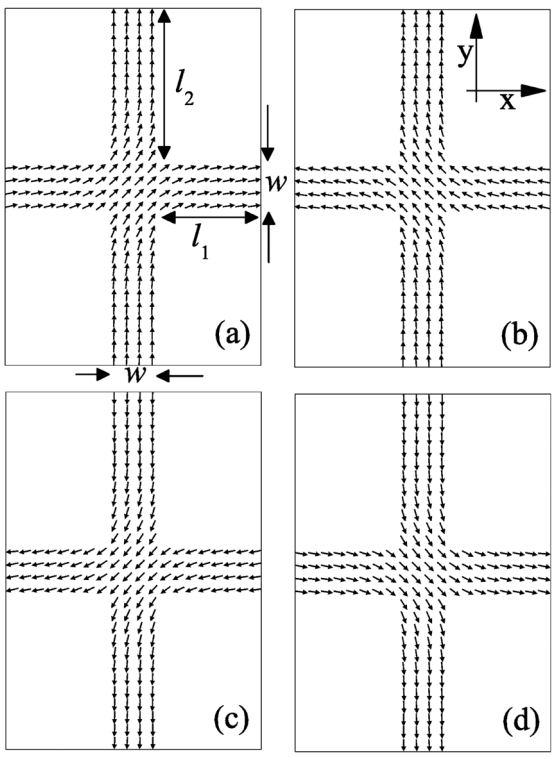

FIG. 1. Equilibrium magnetizations; (a) "State 1"; (b) "State 2"; (c) "State 3"; (d) "State 4"; l_1/w is referred to as AR of short arm, l_2/w is referred to as AR of long arm.

We use the micromagnetic simulator OOMMF[16] to simulate magnetization dynamics of the free layer as a spin-polarized current pulse is applied to it. The Landau-Lifshitz-Gilbert equation is solved with an STT term added

$$\frac{d\vec{m}}{dt} = -|\gamma|\vec{m} \times \vec{H}_{eff} + \alpha\left(\vec{m} \times \frac{d\vec{m}}{dt}\right) + |\gamma|\beta\epsilon(\vec{m} \times \vec{m}_p \times \vec{m}) - |\gamma|\beta\epsilon'(\vec{m} \times \vec{m}_p), \quad (1)$$

where γ = gyromagnetic ratio, α = damping constant, $\vec{m}$ = reduced magnetization, $\beta = |\frac{\hbar}{\mu_0 e}|\frac{J}{tM_s}$, t = free layer thickness, M_s = saturation magnetization, J = charge current density, $\vec{m}_p$ = (unit) polarization direction of the spin-polarized current, $\epsilon = \frac{P\Lambda^2}{(\Lambda^2+1)+(\Lambda^2-1)(\vec{m}.\vec{m}_p)}$, P = spin polarization, and ϵ' = secondary STT term (field-like-torque).

In Eq. (1), ϵ represents the dependence of the spin-polarization on the time-varying free layer magnetization direction $\vec{m}$. In this work, we take Λ to be equal to 1, similar to previous studies[13] for simplicity and assume P to be 0.4. We set ϵ' to 0.06, considering field-like-torque to be 30% of the STT term in Eq. (1).[13] α is taken to be 0.01. $\vec{m}_p$ is taken to be (0.92, 0.382, 0), that is, as mentioned earlier, we assume the fixed layer FM to be pinned making 22.5° angle with the short branch, with its magnetization vector lying in the x-y plane. Also, although the STT acts both on the free layer and the fixed layer, we assume the fixed layer magnetization is pinned by coupling to an adjacent antiferromagnetic layer. We have in mind that the whole MTJ stack has the shape of a cross and the shape and lateral size of the pinned (reference) layer is the same as the shape and size of the free layer, and a uniform spin-polarized current is being injected into the free FM over its entire area. However, with the assumption that the only communication from the fixed layer to the free-layer is via spin-polarized charge injection into the latter, the exact shape and size of the fixed layer are not important for our conclusions, as long as it encompasses the entire area of the free-layer and its magnetization is pinned at a certain angle with respect to the cross.

The magnetization dynamics of the cross is simulated for a negative polarity pulse of amplitude varying from 1×10^7A/cm^2 to 5×10^8A/cm^2 in steps of 5×10^6A/cm^2 to check the effect of STT on the ferromagnetic cross. Cell size for micromagnetic simulation is kept at 1 nm in both directions in plane of the cross, while in out-of-the-plane direction the cell height is equal to the thickness of the FM film, i.e., 2 nm. A smaller cell size in x-y plane does not make any observable difference in the dynamics. The effect of temperature is not considered for simplicity. For all of the dynamic simulations in presence of an injected spin-polarized current, the initial spin distributions are imported from the simulation of the steady state magnetization of "State 1" described in Sec. II.

For a current pulse, the minimum current value at which switching occurs depends on the pulse-width used. The pulse-width has to be larger than the duration of the pre-switching oscillations. By definition, critical switching current density for STT switching is the current density for which small-amplitude oscillations start to grow with time.[17] The 0 crossing time (t_s) for the x-component of spatially

averaged magnetization $\langle m_x \rangle$ for different amplitudes of the negative going current pulse could be fit by[17–19]

$$1/t_s \propto (J - J_{C0}). \tag{2}$$

The curve is extrapolated to find out critical switching current J_{C0}, below which the precession induced by STT is damped by the system. Here, after starting from "State 1," as the system energy increases with time for a $J > J_{C0}$, the system may settle down to either "State 2" or "State 3" after crossing the energy barrier between the stable states. For a low range of current, the system crosses the energy barrier to switch the short branch only and the long branch does not switch. This behaviour is because of the smaller effective shape anisotropy field for the short branch, and asymmetry of the spin polarization direction ($\vec{m}_p$) of the injected current between the branches. If J is greater than J_{C0} (and not too large as is discussed later) switching from "State 1" to "State 2" ($1 \rightarrow 2$ switching) takes place. Therefore, henceforth we will refer to J_{C0} as $J_{1\rightarrow2}$. If the current pulse remains on after $1 \rightarrow 2$ switching takes place, the system attains a steady state magnetization distribution even in the presence of the current (after 6 ns in Figure 2(a)). This result corresponds to the scenario of Eq. (1) with $\frac{d\vec{m}}{dt}$ set to 0. When the current is turned off, the magnetization is damped to the *closest* equilibrium magnetization configuration. As shown in Figure 2, the system is damped to "State 2" after the current pulse is switched off at around 10 ns.

To obtain insight into what defines $J_{1\rightarrow2}$, we repeat this exercise for a set of different ARs of the short branch. For reference, for an elliptic MTJ, the AR tunes the height of the uniaxial energy barrier and hence an effective shape anisotropy field (H_K in Eqs. (1) and (3) in Ref. 19). Similarly, for $1 \rightarrow 2$ switching in the MTJ with the cross-shaped free layer, short arm magnetization flips, so $J_{1\rightarrow2}$ is tuned by the AR of the short branch. Changing the shape of the long branch while keeping the short branch the same does not induce any observable change in $J_{1\rightarrow2}$ (inset of Figure 2(b)).

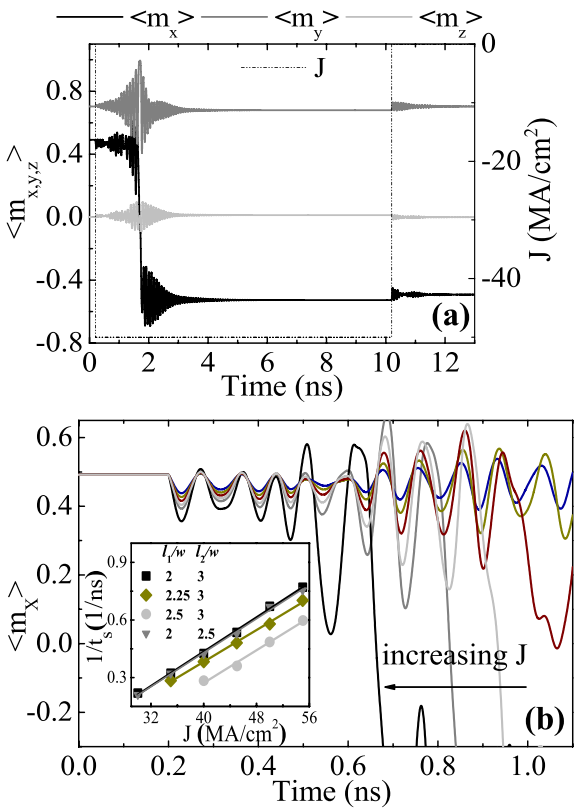

FIG. 2. (a) $1 \rightarrow 2$ switching with $J = 5 \times 10^7 \text{A/cm}^2$. (b) Pre-switching oscillations with different J values; inset: linear fit of 0 crossing time for different values of short branch AR (l_1/w) and long branch AR (l_2/w). l_1, l_2, and w are defined in Figure 1.

For higher current densities, the system undergoes quasi-chaotic dynamics and the final state is almost unpredictable. For example, when viewed as animations, excitations of vortex-like states are observed after the current pulse is turned on, before finally switching to "State 2" for $J = 3.35 \times 10^8 \text{A/cm}^2$ and to "State 3" for $J = 3.4 \times 10^8 \text{A/cm}^2$. This behavior is probably due to excitation of incoherent spin waves but determining the precise J value that triggers this behaviour needs further investigation, perhaps via frequency domain studies with plotting power spectral densities of the spatio-temporal variation of magnetization following methods similar to those of McMichael and Stiles.[20] Similar approaches have been applied to simpler problems of STT-induced magnetization dynamics in ferromagnetic ellipse[21,22] when the macrospin approximation breaks down. Existence of instability region in between deterministic switching regimes has been explained in terms of incoherent spin-wave excitation.[10]

If the current density value is even higher, the long branch also switches and the system settles to "State 3," until the maximum current used in the present work ($5 \times 10^8 \text{A/cm}^2$). This process happens through a systematic sequential switching of the short branch first and then the long branch. A typical switching from "State 1" to "State 3" ($1 \rightarrow 3$ switching) is shown in Figure 3 for $J = 3.8 \times 10^8 \text{A/cm}^2$. Henceforth we refer to the minimum current density for reliable $1 \rightarrow 3$ switching as $J_{1\rightarrow3}$.

"State 4" (Figure 1(d)) cannot be reached by the same polarity of current pulse as could be used to switch to "State 2" and "State 3" from "State 1." A negative polarity of pulse on "State 1" always tries to switch both the branches and $J_{1\rightarrow3} > J_{1\rightarrow2}$. However, using 2 different pulses of opposite polarities consecutively, "State 4" can be reached from "State 1" (Figure 4).

Figure 5 summarizes simulation results of switching for different designs of cross. All the designs have a central

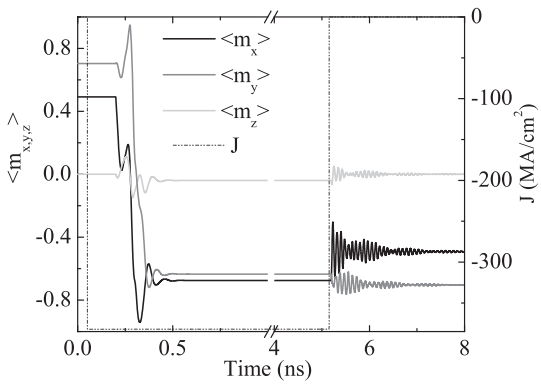

FIG. 3. $1 \rightarrow 3$ switching with $J = 3.8 \times 10^8 \text{A/cm}^2$.

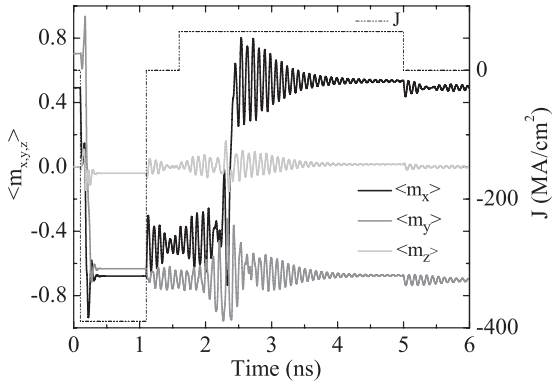

FIG. 4. 1 → 4 switching with two current pulses of opposite polarities and different magnitudes.

square region of 20 nm by 20 nm, with varying lengths of the short and long arms. What we refer to as a "grey" region in which switching is almost random function of the current density is not shown, or rather is shown as breaks in switching current densities, for clarity. These results demonstrate that $J_{1\to3}$ becomes smaller with a smaller AR of long branch for a given width, as can again be understood in terms of the effective shape anisotropy field of the long branch. Figure 5 also provides some insight into design of STT-devices with a biaxial energy landscape (including but perhaps not limited to the cross-shaped free layer devices under consideration here). For a given length of the short arm, if the long arm is made closer in length to the short arm, although $J_{1\to3}$ becomes smaller, monotonic switching regime to "State 2" is observed in an increasingly narrow window, and effectively can be considered to be a part of the grey region for symmetric structure for equal short and long arms.

Critical current density for monodomain switching (J_c) depends on saturation magnetization (M_s) and the damping constant (α).[17,19] We expect similar dependence for the multi-bit scheme studied here. With a reduced α of 0.006, keeping all other material parameters and bit dimensions same, both $J_{1\to2}$ and $J_{1\to3}$ are observed to be reduced. As has been pointed out in previous reports for elliptic magnetic bit (for example, Ref. 19), the main reason for the higher J_c values in in-plane bits compared to bits with perpendicular magnetic anisotropy (PMA) materials, for the same thermal stability, is the extra $2\pi M_s$ term (the in-plane anisotropy) in the expression for J_c. The thermal stability value owing to shape-anisotropy is also effectively decided by M_s, for a given dimension of the bit. The multi-bit structure considered here also is subject to the switching current density versus thermal stability trade-off. Trying to exploit the effect of shape anisotropy to have more than one easy axis, the scheme suffers from the inherent disadvantage of in-plane magnetized magnetic bit as compared to using, for example, material with PMA. As has been verified with simulations, attempt to decrease $J_{1\to2}$ and $J_{1\to3}$ by decreasing M_s, for a given value of α and the dimensions of the cross, will result in a compromise in thermal stability.

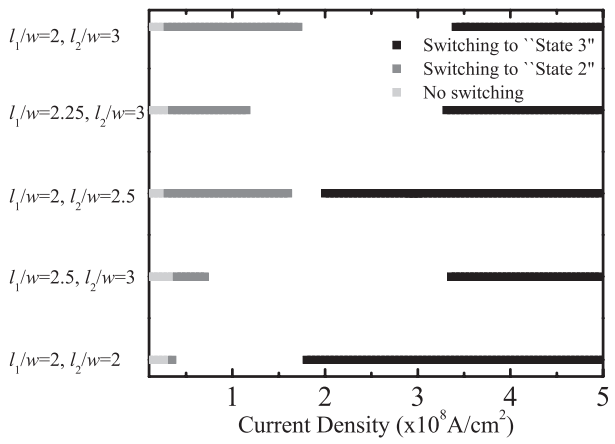

FIG. 5. Switching regions to "State 2" and "State 3" starting from "State 1" with increasing amplitude of current pulse in steps of $J = 5 \times 10^6 \mathrm{A/cm^2}$ for different designs of cross.

Moreover, the efficiency of spin-filtering by the tunnel barrier between the free and fixed layers, that is, tunneling spin polarization (TSP) of the current injected to the free layer is also expected to tune critical switching current density, as has been studied already experimentally.[24] Larger TSP should lead to lower value of J_c for an elliptic bit, as was predicted by the macrospin-model.[17] Here, we assume a rather conservative value of P (in Eq. (1)) of 0.4. Assumption of higher P leads to lower values of $J_{1\to2}$ and $J_{1\to3}$, as has been verified by simulations.

IV. THERMAL STABILITY

Thermal stability of a STTRAM bit is an important consideration, often setting a trade-off between maximum storage density achievable and the requirement for data retention, where the latter requires an energy barrier of about $60k_BT$ (k_B is Boltzmann's constant and T is absolute temperature) for 10 year retention.[19] In general, a magnet might not switch under thermal fluctuation as a mono-domain. That is, spins might not be parallel to each other while switching. In that case, there will be another contribution to the energy barrier, the exchange energy.[23] The total barrier will depend on the path the system takes in the phase-space while thermally switching. To estimate the thermal stability of the bit, we follow a method similar to that reported for stability calculations for an elliptic magnet.[23] Starting from "State 1," a large magnetic field (500 mT) is applied along the y axis to saturate the magnetization along the hard axis of the short branch. The difference of the demagnetization energy in these two states is estimated to be the energy barrier due to shape anisotropy for the system to go from "State 1" to "State 2" for in-plane rotation under thermal fluctuation. That is, we ignore the contribution due to exchange energy while switching. For the cross with a 20 nm by 20 nm center, and branches with ARs of 2 and 3, this energy is approximately equal to $62.7k_BT$ at $T = 300$ K. As the short branch has a smaller energy barrier, this energy barrier limits the bit's stability against in-plane rotation of magnetization under thermal activation. We have not discussed simulation results on smaller cross sizes than this (i.e., smaller center sizes while keeping the aspect ratios the same) as these are not expected to be thermally stable according to the $60k_BT$ energy barrier benchmark.

V. CONCLUSION

We have studied STT switching of a ferromagnet with an energy landscape that is effectively biaxial, in contrast with conventional MTJs with elliptic cross-section where the shape defines an effective uniaxial potential profile. We demonstrated that by introducing asymmetry (here by the combined effect of the spin polarization direction and the ARs of the arms of the cross), monotonic regions of switching with increasing spin-polarized current density can be achieved. The results potentially could be used towards storing more than one memory bit in a single MTJ-like structure for improved storage density.

ACKNOWLEDGMENTS

This work was supported in part by the NSF NNIN and NSF NASCENT ERC center. We thank Michael Donahue for help on OOMMF. M.T. is supported in part by NSF Grant DMR 1207577.

[1]J. Slonczewski, "Current-driven excitation of magnetic multilayers," J. Magn. Magn. Mater. **159**, L1–L7 (1996).
[2]L. Berger, "Emission of spin waves by a magnetic multilayer traversed by a current," Phys. Rev. B **54**, 9353–9358 (1996).
[3]M. Tsoi, A. G. M. Jansen, J. Bass, W.-C. Chiang, M. Seck, V. Tsoi, and P. Wyder, "Excitation of a magnetic multilayer by an electric current," Phys. Rev. Lett. **80**, 4281–4284 (1998).
[4]*Handbook of Spin Transport and Magnetism*, edited by E. Y. Tsymbal and I. Žutić (Chapman and Hall/CRC, 2012).
[5]P. K. Amiri and K. L. Wang, "Voltage-controlled magnetic anisotropy in spintronic devices," SPIN **02**, 1240002 (2012).
[6]D. V. Dimitrov, Z. Gao, and X. Wang, U.S. patent 783,438,5 (2010).
[7]T. Ishigaki, T. Kawahara, R. Takemura, K. Ono, K. Ito, H. Matsuoka, and H. Ohno, "A multi-level-cell spin-transfer torque memory with series-stacked magnetotunnel junctions," in *2010 Symposium on VLSI Technology (VLSIT)* (IEEE, 2010), pp. 47–48.
[8]X. Lou, Z. Gao, D. V. Dimitrov, and M. X. Tang, "Demonstration of multilevel cell spin transfer switching in MgO magnetic tunnel junctions," Appl. Phys. Lett. **93**, 242502 (2008).
[9]J. L. Leal and M. H. Kryder, "Spin valves exchange biased by Co/Ru/Co synthetic antiferromagnets," J. Appl. Phys. **83**, 3720–3723 (1998).
[10]Y. Zhou, J. Åkerman, and J. Z. Sun, "Micromagnetic study of switching boundary of a spin torque nanodevice," Appl. Phys. Lett. **98**, 102501 (2011).
[11]J. A. Osborn, "Demagnetizing factors of the general ellipsoid," Phys. Rev. **67**, 351–357 (1945).
[12]I. N. Krivorotov, D. V. Berkov, N. L. Gorn, N. C. Emley, J. C. Sankey, D. C. Ralph, and R. A. Buhrman, "Large-amplitude coherent spin waves excited by spin-polarized current in nanoscale spin valves," Phys. Rev. B **76**, 024418 (2007).
[13]D. E. Nikonov, G. I. Bourianoff, G. Rowlands, and I. N. Krivorotov, "Strategies and tolerances of spin transfer torque switching," J. Appl. Phys. **107**, 113910 (2010).
[14]C.-Y. You, "Reduced spin transfer torque switching current density with non-collinear polarizer layer magnetization in magnetic multilayer systems," Appl. Phys. Lett. **100**, 252413 (2012).
[15]U. Roy, H. Seinige, F. Ferdousi, J. Mantey, M. Tsoi, and S. K. Banerjee, "Spin-transfer-torque switching in spin valve structures with perpendicular, canted, and in-plane magnetic anisotropies," J. Appl. Phys. **111**, 07C913 (2012).
[16]M. J. Donahue and D. G. Porter, OOMMF User's Guide, Report No. NISTIR 6376 (National Institute of Science and Technology, 1999).
[17]J. Z. Sun, "Spin-current interaction with a monodomain magnetic body: A model study," Phys. Rev. B **62**, 570–578 (2000).
[18]Z. Li and S. Zhang, "Magnetization dynamics with a spin-transfer torque," Phys. Rev. B **68**, 024404 (2003).
[19]D. Apalkov, S. Watts, A. Driskill-Smith, E. Chen, Z. Diao, and V. Nikitin, "Comparison of scaling of in-plane and perpendicular spin transfer switching technologies by micromagnetic simulation," IEEE Trans. Magn. **46**, 2240–2243 (2010).
[20]R. D. McMichael and M. D. Stiles, "Magnetic normal modes of nanoelements," J. Appl. Phys. **97**, 10J901 (2005).
[21]K.-J. Lee, A. Deac, O. Redon, J.-P. Nozires, and B. Dieny, "Excitations of incoherent spin-waves due to spin-transfer torque," Nature Mater. **3**, 877–881 (2004).
[22]C.-M. Lee, J.-S. Yang, and T.-H. Wu, "Micromagnetic simulation for spin-transfer switching with a tilted spin polarizer," IEEE Trans. Magn. **47**, 649–652 (2011).
[23]S. Hoffman, Y. Tserkovnyak, P. K. Amiri, and K. L. Wang, "Magnetic bit stability: Competition between domain-wall and monodomain switching," Appl. Phys. Lett. **100**, 212406 (2012).
[24]Z. Diao, D. Apalkov, M. Pakala, Y. Ding, A. Panchula, and Y. Huai, "Spin transfer switching and spin polarization in magnetic tunnel junctions with MgO and AlOx barriers," Appl. Phys. Lett. **87**, 232502 (2005).